Online Four Dimensional Trajectory Prediction Method based on Aircraft Intent Updating

Junfeng ZHANG*, Jie LIU, Rong HU, Haibo ZHU

College of Civil Aviation, Nanjing University of Aeronautics and Astronautics, Nanjing 210016, China

ABSTRACT: To facilitate decision support in the air traffic management domain, an online four dimensional trajectory prediction (4D-TP) method was proposed in this paper. First, this study outlined the processes of online 4D-TP. Second, four major components of offline 4D-TP were discussed and presented, such as computation model, aircraft intent, environmental conditions and performance parameters. Third, this paper came up with an approach of current trajectory updating by using ADS-B Receiver and the corresponding data processing algorithm. Furthermore, the strategies of aircraft horizontal and vertical intent updating were also put forward for online 4D-TP. And the aircraft intent should be updated while the deviation between the current and predicted trajectory exceeding the pre-defined threshold. Finally, two types of case studies were carried out to demonstrate the performance and effectiveness of the proposed online 4D-TP method. The results indicated that the proposed online 4D-TP method is able to increase the prediction accuracy by triggering 4D-TP while the position or speed deviation is beyond the pre-defined threshold.

Keywords: Trajectory Prediction; Air Traffic Management; Aircraft Intent; ADS-B

1. INTRODUCTION

Currently, the Air Traffic Management (ATM) relies on a set of operational measures for air traffic to fulfill the missions of separating, metering and sequencing [1]. The ever continuous growth and still increasing demand of air transport are posing significant challenges to the civil aviation community; as such current paradigms of ATM will not ensure the target levels of safety, capacity, efficiency and environmental sustainability in the future. As a consequence, several renovation projects have been launched, such as the Single European Sky ATM Research (SESAR) in Europe, the Next Generation Air Transportation System (NextGen) in the United States, and the Aviation System Block Upgrades (ASBU) framework from International Civil Aviation Organization (ICAO), to enhance the levels of safety, capacity, efficiency and environmental sustainability. In the ATM domain, conflict detection and resolution [2], aircraft sequencing and scheduling [3], trajectory based operation [4] are the most promising novel concepts and advanced technologies of the above renovation projects. And these concepts and technologies could not be implemented without the accurate Four Dimensional Trajectory Prediction (4D-TP).

4D Trajectory Prediction is the process that estimates a future 4D trajectory (in three spatial dimensions, i.e., latitude, longitude and altitude, plus time dimension) of individual aircraft through computation [5] on the basis of current aircraft states, estimated pilot's and/or controller's intent, expected environmental conditions and computer models of aircraft performance and procedures. Besides the definition of 4D-TP, FAA/Eurocontrol Action Plan 16 (Common Trajectory Prediction Capabilities) also proposed varied performance requirements, like accuracy, uncertainty and response times. More specifically, an important conclusion was put forward in Action Plan 16 that the structure, process, function and performance requirements of 4D-TP were totally dependent on the application of 4D-TP, which was to say that 4D-TP for conflict detection, conflict resolution, aircraft sequencing, or flight planning had different concerns. However, the key issue of 4D-TP seems obvious that how to quickly and accurately predict 4D trajectory. Many researchers have devoted themselves to addressing this issue.

*Corresponding author at: College of Civil Aviation, NUAA, Nanjing, 210016, China. Tel.: +8613851944772.
E-mail address: zhangjunfeng@nuaa.edu.cn (J-F. ZHANG).

Trajectory prediction is the process of estimating a future trajectory for an individual aircraft, thus the optimal estimation is a reliable method for 4D-TP. Additionally, the aircraft movement involves both continuous dynamics and discrete modes switching, then trajectory prediction can be viewed as a hybrid estimation problem which may be tackled with multiple-model methods. And the Interacting Multiple Model (IMM) algorithm is a case in point [6]. In order to produce better mode and state estimates, Hwang [7] proposed a modified version of the IMM algorithm, called the Residual-Mean Interacting Multiple Model (RMIMM) algorithm, based on a new likelihood function. But the RMIMM algorithm still followed the assumption of residuals being zero mean, only considered the characteristics of single Kalman filter's residual and casually neglected the mixing process in the standard IMM algorithm. In view of these, Zhang [8] presented a new method for updating flight mode probabilities, which discarded the zero mean residual assumption and took the interacting influences into account. Furthermore, in the ATM domain, an aircraft always flies over the air routes, thereupon the transition probabilities of flight modes can be modeled as a state-dependent Markov process. As a result, Seah and Hwang [9] proposed the State-Dependent Transition Hybrid Estimation (SDTHE) algorithm for trajectory tracking and predicting to infer aircraft intent [10] and detect potential conflict [11]. Zhang [12] presented the SDTHE algorithm based on [8] to improve the accuracy of mode estimation and trajectory prediction.

Kinematic and kinetic modeling is another important method to implement trajectory prediction on the basis of current aircraft states, estimated aircraft intent, expected environmental conditions and aircraft performance parameters. In other words, this method consists of four distinctive parts: computation model, aircraft intent, environmental conditions and performance parameters. As to computation model, Total Energy Model (TEM) [13] and Point-Mass Model (PMM) [14] are most extensively applied. Zammit and Mangion [15] addressed the suitability of TEM for fast trajectory prediction during idle-thrust descents. PMM was utilized for trajectory optimization [16,17] by means of hybrid optimal control strategy. In terms of TEM, the energy sharing factor was a huge hurdle for trajectory prediction. As regards aircraft intent, the Aircraft Intent Description Language (AIDL) [18,19] was the most reliable way, which provided necessary elements to unambiguously formulate the aircraft intent. And the lateral, altitude and speed constraints could be extracted from the radar tracks, the procedures of airlines and the transfer agreements between different sectors. As for the environmental conditions, especially wind field, they can be obtained through meteorological observation and forecast [20], or local wind vector estimation with spatial and temporal variations [21]. With regard to the performance parameters, BADA [13] were widely used for the parameters of flight envelope, aerodynamics, engine thrust and fuel flow. The international Aircraft Noise and Performance database (ANP) [22] would be an alternative.

With the development of "Big Data" research in the ATM field, the machine learning method is an essential supplement to the trajectory prediction, especially for the flight time estimation field. On the one hand, it is dependent on the similarity of trajectories, while only taking past radar tracks into account. Hong and Lee [23] introduced a new framework for predicting arrival times by incorporating probabilistic information for the identified trajectory patterns. Tastambekov et.al [24] put forward an innovative approach for the trajectory prediction based on the local linear functional regression that considered data preprocessing, localizing and solving linear regression using wavelet decomposition. On the other hand, it is based on the reconstruction of input and output space. Leege [25] brought forward machine learning approach for the trajectory prediction based on the historic aircraft trajectory and meteorological data.

As discussed above, there exist three main methods for trajectory prediction: optimal estimation, kinematic and kinetic modeling and machine learning. And these methods have been widely used to predict the future trajectory, and moreover, to facilitate decision support in the ATM domain. So far, however, there has been little discussion about online trajectory prediction. With reference to this aspect of the research achievements, Alligier [26, 27] made the best of the past observations to estimate mass

and thrust parameters so as to improve the prediction accuracy. Nevertheless, such studies only focused on the proper updates of several parameters.

This paper aims at developing an online 4D-TP method. We firstly acquire the current surveillance messages of the aircraft through Automatic Dependent Surveillance - Broadcast (ADS-B) receiver. Secondly, we decode those surveillance messages to obtain the flight states of the aircraft and compare them with the predicted trajectory. Thirdly, if the deviation between current flight states and predicted trajectories beyond a threshold, then the aircraft horizontal intent and vertical intent updating methods are triggered. Finally, based on the updated aircraft intent and current states, we carry out the 4D-TP.

The novelty of the proposed online 4D-TP method is two-fold: First, the accessible current trajectory from ADS-B receiver could help to fulfill the function of trajectory conformance monitoring, which is served as a trigger for online 4D-TP. Second, the accessible current trajectory from ADS-B receiver is fully used to design the aircraft horizontal and vertical intent updating methods for online 4D-TP. Such proposed method might help to enhance the function and improve the accuracy of trajectory prediction to facilitate decision support in the ATM domain.

This paper is organized as follows: First, an online 4D-TP problem is addressed in Section 2. Subsequently, section 3 details the model and method of online 4D trajectory prediction. The simulation and validation results are presented and discussed in Section 4, before the conclusion in Section 5.

2. PROBLEM FORMULATION

As trajectory prediction is the process of estimating a future trajectory for an individual aircraft, online 4D-TP needs to update the future trajectory estimation in response to several events such as availability of new constraint information or deviation between actual and predicted trajectory exceeding a predefined threshold. Thereupon, our proposed online 4D-TP method is composed of three processes: preparation, computation and updating. The process flow chart of online 4D-TP is shown in Figure 1, which is derived from Ref. [5].

Meteorological data, aircraft performance data and adaption data provide support function for the 4D-TP, in which adaption data consists of control airspace, control sectors, air routes, standard instrument departure (SID) and standard terminal arrival route (STAR).

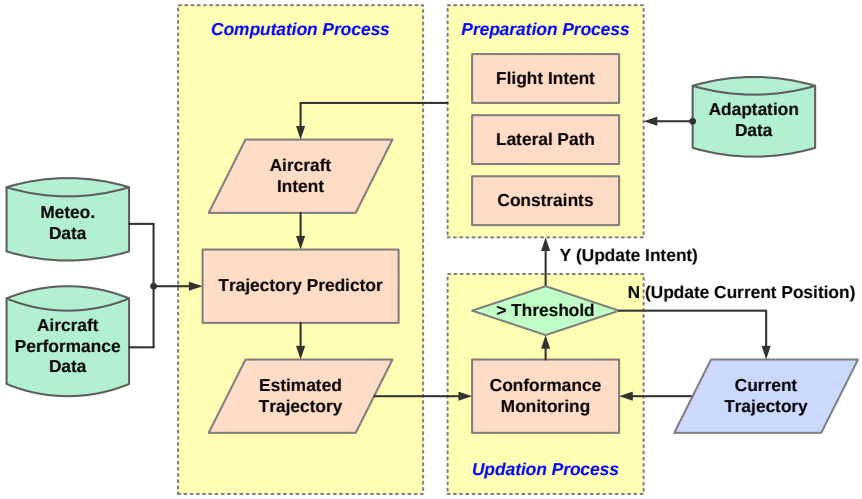

Figure 1 Process flow chart of online trajectory prediction

Preparation process creates the initial version of flight intent based on flight plan and adaptation data. This process is activated at the beginning or when the trajectory prediction should be updated. Computation process constitutes the kernel function of 4D-TP, in which the aircraft intent contains a

description of the way the aircraft will be operated, the trajectory predictor integrates aircraft intent information into 4D trajectory using the atmospheric conditions and the aircraft performance parameters, and estimated trajectory serves as the output of 4D-TP. For online 4D-TP, updating process plays an important role, which may result in the generation of new aircraft intent by triggering preparation process again and again. Conformance monitoring [28-30] in the updating process aims at determining whether the re-prediction is required or not. In this paper, conformance monitoring depends on the deviation between predicted trajectories and current states exceeds the pre-defined threshold whether or not.

The current trajectory offers a baseline for conformance monitoring to trigger the online 4D-TP whether or not. In this paper, the current trajectory was obtained through the ADS-B receiver (BAR6216 ADS-B 1090MHZ Receiver).

3. MODEL AND METHOD

3.1 4D Trajectory Prediction Model

3.1.1 Computation model

Even though Point-Mass Model (PMM) does not reflect all the intricacies of an aircraft movement, it is reasonably accurate and very commonly used in the ATM research field. Figure 2 summarizes the major variables of a PMM for an aircraft movement: The horizontal position (x and y) and altitude (h) of the aircraft, the True Airspeed (V_{TAS}), the flight path angle (γ), heading angle (ψ) and bank angle (ϕ). The forces applied to the aircraft are its weight (mg), the engine thrust (T), and the aerodynamic forces of lift (L) and drag (D). The aerodynamic forces depend on the angle of attack (α) and the side slip angle (β).

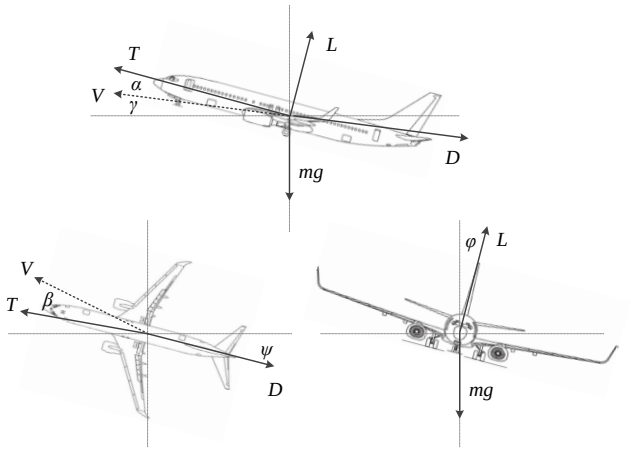

Figure 2 Diagram of forces acting on an aircraft

From the point of view of the ATM field, we can assume trimmed flight conditions, $\alpha = \beta = 0$, ignore fast dynamics, and treat γ, T and ϕ as inputs. Thus, the PMM of an aircraft movement becomes:

$$\begin{aligned} \dot{x} &= V_{\mathrm{TAS}} \sin(\psi)\cos(\gamma) + w_1 \\ \dot{y} &= V_{\mathrm{TAS}} \cos(\psi)\cos(\gamma) + w_2 \\ \dot{h} &= V_{\mathrm{TAS}} \sin(\gamma) \\ \dot{V}_{\mathrm{TAS}} &= (T - D)/m - g\sin(\gamma) \\ \dot{\psi} &= g\tan\phi / V_{\mathrm{TAS}} \\ \dot{m} &= -\eta T \end{aligned} \tag{1}$$

where w_1 and w_2 are the east-trending and north-trending wind velocity components respectively, and η is a thrust-specific fuel consumption parameter.

3.1.2 Performance parameters

The BADA model [13] provides parameters for the following three thrust levels: maximum climb and take-off; maximum cruise and descent.

The drag is calculated through multiplying the drag coefficient C_D by dynamic pressure and wing surface area S:

$$D = \frac{1}{2} C_D \cdot \rho \cdot V_{\mathrm{TAS}}^2 \cdot S \tag{2}$$

where ρ is atmospheric density and C_D is specified as a function of the lift coefficient C_L as follows:

$$C_D = C_{D0,\,\mathrm{Config.}} + C_{D2,\,\mathrm{Config.}} \cdot (C_L)^2 \tag{3}$$

where the subscript "Config." represents the different aircraft configurations: such as take-off, climb, cruise, approach and landing configurations. The lift coefficient, C_L, is determined through the correction of bank angle (ϕ) and flight path angle (γ).

$$C_L = \frac{2 \cdot m \cdot g_0 \cdot \cos\gamma}{\rho \cdot V_{\mathrm{TAS}}^2 \cdot S \cdot \cos\phi} \tag{4}$$

3.1.3 Aircraft intent

Aircraft intent is defined as a set of instructions that are provided as inputs to a computation model in order to specify how the aircraft is to be operated for the 4D-TP. In general, these instructions capture the basic commands and guidance modes at the disposal of the pilot/Flight Management System (FMS) to direct the operation of the aircraft [18].

Depending on the degrees of freedom (DOFs) being affected, any instruction belongs to one of the following groups: speed, altitude, thrust or lateral. In this paper, speed instructions define airspeed profile, altitude instructions represent altitude profile, thrust instructions denote thrust setting profile and lateral instructions indicate horizontal track. The former three groups of instructions are used to elaborate how the aircraft is to be operated in its vertical motion, while the last group of instructions describes its lateral motion. Table 1 lists the different groups, detailed instructions, constraint categories and affecting parameters of the aircraft intent model.

Table 1 Tabulation of aircraft intent model

Group	Instruction	Category	Parameters
Speed	*Hold CAS*	Kinematic constraints	V_{CAS}
	Hold Mach		*Mach*
	Hold ROCD		$\dot{h}$
Altitude	*Hold Altitude*	Geometric constraints	h
	Hold Flight Path		γ
Thrust	*Idle, Climb, Cruise*	Kinematic constraints	T
Lateral	*Hold Track*	Geometric constraints	ψ
	Hold Turn Rate	Kinematic constraints	ϕ

3.1.4 Environmental conditions

Environmental conditions modeling involve the estimation of atmospheric properties (pressure, temperature, density and speed of sound) and wind field (wind speed and direction) at different related areas and flight levels. The atmospheric properties can be estimated as a function of flight altitude [13], while the wind field can be obtained from European Centre for Medium-Range Weather Forecasts (ECMWF), which provides the most accurate medium-range global weather forecasts to 15 days.

The wind field, provided by ECMWF, is in GRIB-II format, which is a concise data format commonly used in meteorology to store the historical and forecast weather data. The main steps in the wind field generation for 4D-TP are retrieving and interpreting data in GRIB-II format. The data retrieving step includes the determination of region, pressure layers, date, time (0h 6h 12h 18h UTC), meteorological parameters (*u* wind, *v* wind, temperature), and grid resolution (0.75°×0.75°). The data interpreting step is displayed in detail in Figure 3, in which the wind field at particular time and waypoint can be obtained through spatio-temporal interpolation.

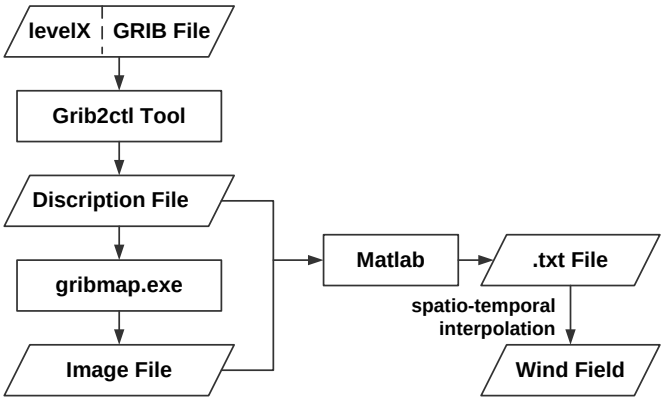

Figure 3 Diagram of GRIB format data interpreting step

The spatio-temporal interpolation of the wind field plays a key role in the environmental conditions modeling. The first step is to select the times of weather forecast, which should be close to the current time. Then two group of the wind field information are obtained. In each group, the tridimensional grids with eight vertices, adjacent to the current position, are chosen to be used in the interpolation, as shown in Figure 4. Afterwards, the three-dimensional linear interpolation method is adopted to get the wind field information at current position (red circle in Figure 4). Finally, linear interpolation is used again in the light of different group of weather forecast time to get the wind field information at the current position and current time.

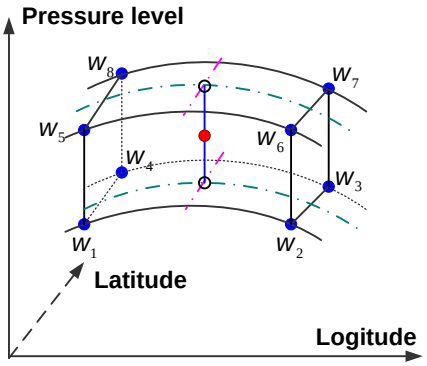

Figure 4 Tridimensional grids with eight vertices of wind field

The wind speed V_{wind} and wind direction φ_{wind} at particular time and position can be calculated by using the following equations:

$$V_{\text{wind}} = \sqrt{u^2 + v^2} \tag{5}$$

$$\varphi_{\text{wind}} = \begin{cases} \arctan(u/v) & u > 0, v > 0 \\ 180 - \arctan(u/-v) & u > 0, v < 0 \\ 180 + \arctan(-u/-v) & u < 0, v < 0 \\ 360 - \arctan(-u/v) & u < 0, v > 0 \end{cases} \tag{6}$$

3.2 Current Trajectory Updating Method

For online 4D-TP, the updating process plays a key role, which comprises the tasks of current trajectory updating and aircraft intent updating. This subsection mainly deals with the former task, to provide available current trajectory. The provision of available current trajectory consists of the following steps: message receiving, decomposing and decoding, as shown in Figure 4.

Firstly, an ADS-B Receiver (BAR6216 ADS-B 1090MHZ Receiver) is employed to receive the message streams which are broadcasted from aircraft in TCP Protocol. Such message streams contain the information sent by all aircraft within the coverage of the ADS-B Receiver.

Subsequently, decomposition step is implemented to obtain the message of every aircraft. As can be seen from Figure 5, through Wireshark, every line represents a message, which indicates the one kind of particular flight information (in HEX format) of a particular aircraft.

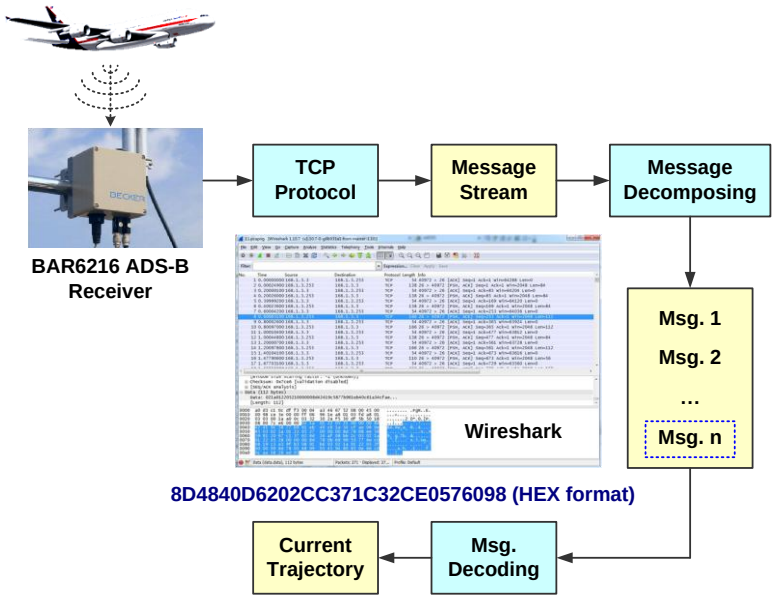

Figure 5 Diagram of processing steps for current trajectory updating

Table 2 Meanings of each field of 112 bits data packets

Bit from	Bit to	Abbr.	Name
1	5	DF	Downlink Format
6	8	CA	Message Subtype
9	32	ICAO24	ICAO aircraft address
33	88	DATA	Data frame
89	112	PC	Parity check

Finally, message decoding should be carried out to determine the identification, position and velocity of every aircraft within the coverage of ADS-B Receiver. Prior to this, HEX format of each message needs to be converted to Binary format so that each message is composed of 112 bits. Table 2 presents the meaning of each field of data packets.

The following cases illustrate how to determine the flight identification, position and velocity of every aircraft based on the 112 bits data packets, as shown in Figure 6.

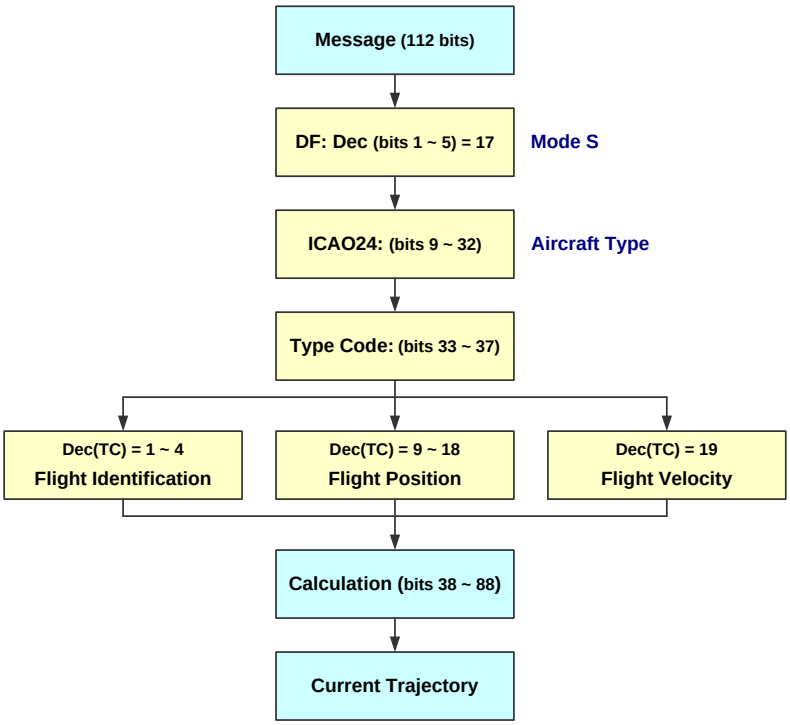

Figure 6 Diagram of message decoding for current trajectory updating

(1) If the type of message (33rd-37th bit) is between 1 to 4, this message indicates the Flight Identification. Convert the 41st-88th bits from Binary format into Decimal format, and obtain the Flight Identification.

(2) If the type of message (33rd-37th bit) is between 8 to 19, this message indicates the Flight Position. In order to obtain the Flight Position, the Compact Position Reporting (CPR) algorithm should be used for decoding [31].

(3) If the type of message (33rd-37th bit) is 19, this message indicates the Flight Velocity. In order to obtain the Flight Velocity, four kinds of information are needed for calculation, such as: East-West Direction Index (57th bit), East-West Speed (58th-67th bit), North-South Direction Index (46th bit) and North-South Speed (47th-56th bit).

3.3 Aircraft Intent Updating Method

For online 4D-TP, current trajectory is employed to fulfill the function of the trajectory conformance monitoring. In turn, the trajectory conformance monitor acts as a trigger to generate new aircraft intent or not. If the deviation between current states and predicted trajectory exceeds the pre-defined threshold, new aircraft intent is generated and trajectory re-prediction is required. If not, keep on updating current trajectory. Figure 7 illustrates the whole process.

If the trajectory re-prediction is triggered, the historical and current trajectories should be fully utilized to generate new aircraft intents, including aircraft horizontal intent and vertical intent.

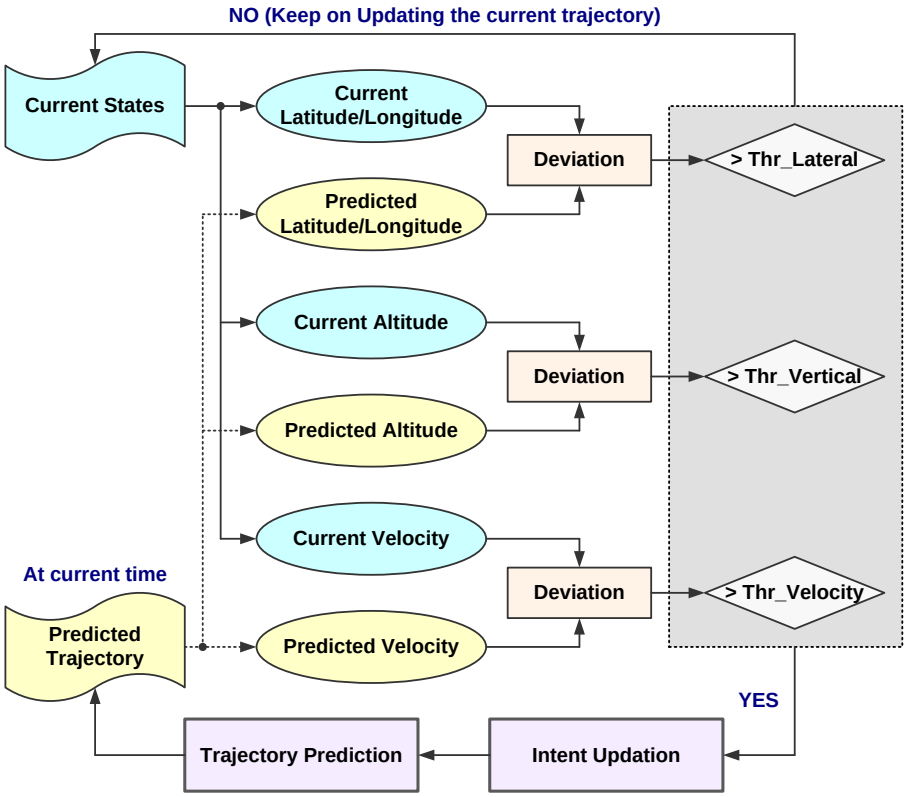

Figure 7 Diagram of the whole process of online trajectory prediction

As far as aircraft horizontal intent updating strategy is concerned, this paper takes advantage of the distances and angles between current position and the waypoints along Air Route or SID or STAR. Figure 8 provides aircraft horizontal intent updating strategy within the arrival context, where STAR is defined as a series of waypoints (WPs) from WP1 to WP5.

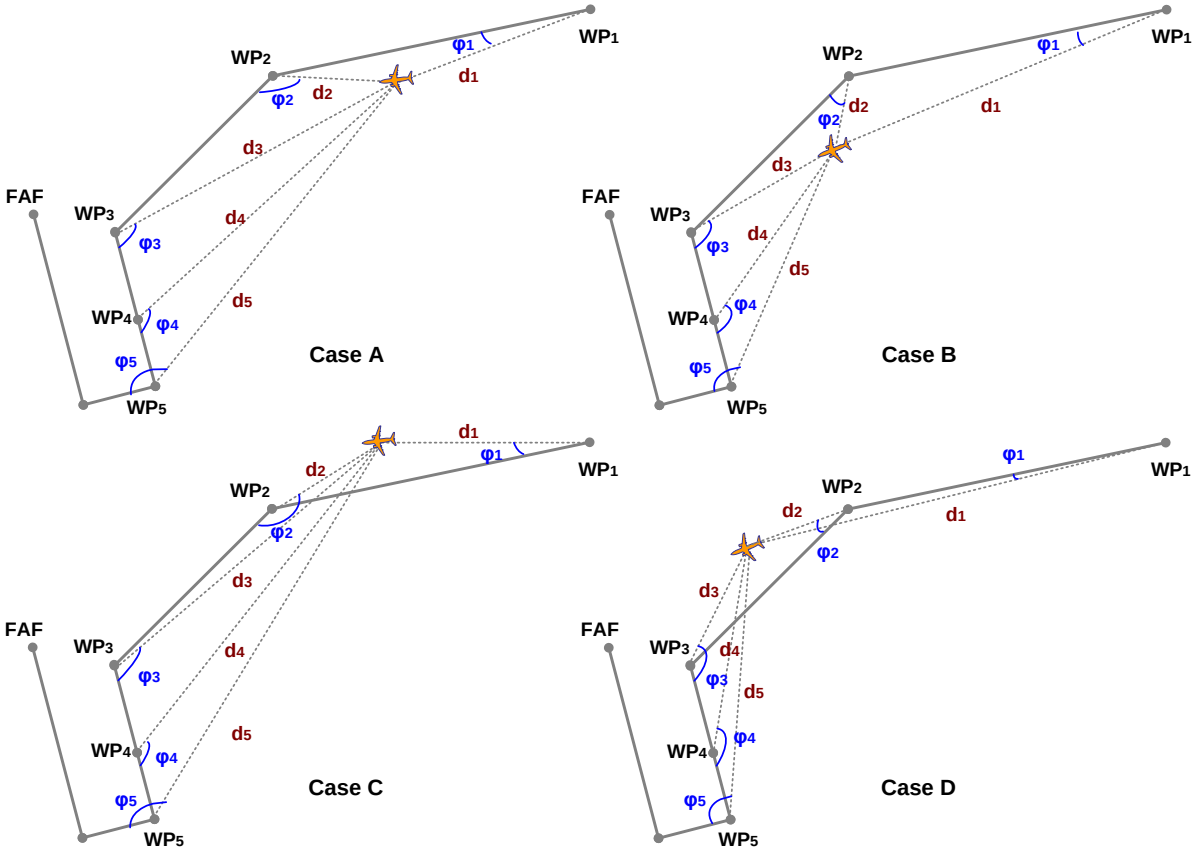

Figure 8 Diagram of the horizontal aircraft intent updating strategy

As shown in Figure 8, aircraft horizontal intent updating strategy is composed of the following steps:

Firstly, calculate the distances (d_i,) and angles (φ_i) between current position and the waypoints along STAR. φ_i is less than 180 degree without considering the clockwise and counterclockwise directions.

Secondly, find the nearest waypoint, where WP_2 is the case in Figure 8. And compare the angle of such nearest waypoint with 90 degree. If the angle is higher than 90 (Case A/C), it means that the aircraft should fly to such waypoint. Otherwise (Case B/D), it means that the aircraft has passed such waypoint.

Thirdly, trigger the preparation process and update the altitude and speed constraints at every waypoint to be passed subsequently based on the current altitude/speed, in which the conversion of Ground Speed (GS) to True Air Speed (TAS) and Calibrated Air Speed (CAS) are needed.

$$V_{\mathrm{TAS}} = \left(V_{\mathrm{GS}} - V_{\mathrm{wind}} \cdot \cos\left(\varphi_{\mathrm{WA}}\right)\right) / \cos\left(\varphi_{\mathrm{DA}}\right) \tag{7}$$

where $\varphi_{\mathrm{WA}} = \varphi_{\mathrm{wind}} - MC$, φ_{WA} denotes the wind angle and MC denotes the magnetic course; $\varphi_{\mathrm{DA}} = \arcsin\left(V_{\mathrm{wind}} / V_{\mathrm{TAS}} \cdot \sin\left(\varphi_{\mathrm{WA}}\right)\right)$, φ_{DA} denotes the drift angle.

$$V_{\mathrm{CAS}} = \left[\frac{2\kappa}{\kappa-1}\frac{p_0}{\rho_0}\left\{\left(1+\frac{p}{p_0}\left[\left(1+\frac{\kappa-1}{2\kappa}\frac{\rho}{p}V_{\mathrm{TAS}}^2\right)^{\frac{\kappa}{\kappa-1}}-1\right]\right)^{\frac{\kappa-1}{\kappa}}-1\right\}\right]^{\frac{1}{2}} \tag{8}$$

where $\kappa = 1.4$, κ denotes the adiabatic index of air; $p_0 = 101325$ Pa, p_0 denotes the standard atmospheric pressure at Mean Sea Level (MSL); $\rho_0 = 1.225$ kg/m^3, ρ_0 denotes the standard atmospheric density at MSL; p and ρ denote the atmospheric pressure and density at particular altitude, respectively.

As far as aircraft vertical intent updating strategy is concerned, this paper takes advantage of the vertical profile of the historical 4D trajectories. And the aircraft vertical intent updating strategy is composed of the following steps:

Firstly, calculate the rate of climb or descent (ROCD, i.e. $\dot{h}$) and CAS (V_{CAS}) according to Equation (7) and (8) based on the historical vertical profiles and wind field information.

Secondly, if ROCD is nearly constant, the aircraft vertical intent of climbing or descending while holding ROCD is selected. If CAS is nearly constant, the aircraft vertical intent of climbing or descending while holding CAS is selected.

Thirdly, if the updating vertical intent is climbing or descending while holding ROCD, then $\dot{h}$ in Equation (1) is replaced by $\dot{h}$=ROCD. If the updating vertical intent is climbing or descending while holding CAS, then $\dot{h}$ in Equation (1) is replaced by Energy Sharing Factor form, which is elaborated in [13].

After updating the aircraft horizontal and vertical intent, re-generate the whole aircraft intent and re-predict the trajectory based on the 4D Trajectory Prediction Model described in subsection 3.1.

4. SIMULATION AND DISCUSSION

In this section, two types of case studies were carried out to demonstrate the performance and effectiveness of the proposed 4D-TP method. At the beginning, offline 4D-TP method was validated by radar tracks obtained from ATM system for departure aircraft. After that, online 4D-TP method was verified by the available current trajectory obtained from ADS-B receiver for arrival aircraft. Moreover, the results were discussed at the end of each subsection.

In the simulation, the "reference mass" in BADA was used for the arrival 4D-TP method. As far as departure was concerned, the mass was determined by the "maximum mass" multiplying a coefficient based on the range of operation and the analysis of the Quick Access Recorder (QAR) data.

4.1 Offline 4D-TP Case Study

In this case, we took Shanghai Pudong airport (ZSPD) into consideration. And the operational scenario is shown in Figure 9. Figure 9(a) presented the SIDs, STARs and sectorization around ZSPD airport, in which the grey lines represented the sectorizaiton of Terminal Area (TMA), the blue and red dotted lines represented SIDs and STARs, respectively. Figure 9(b) displayed radar tracks on a particular day (Jan. 2nd, 2013) in the TMA, in which the blue and red lines denoted the departure and arrival trajectories, respectively. From Figure 9(b), we could find that the approach of radar vectoring was frequently used in the TMA.

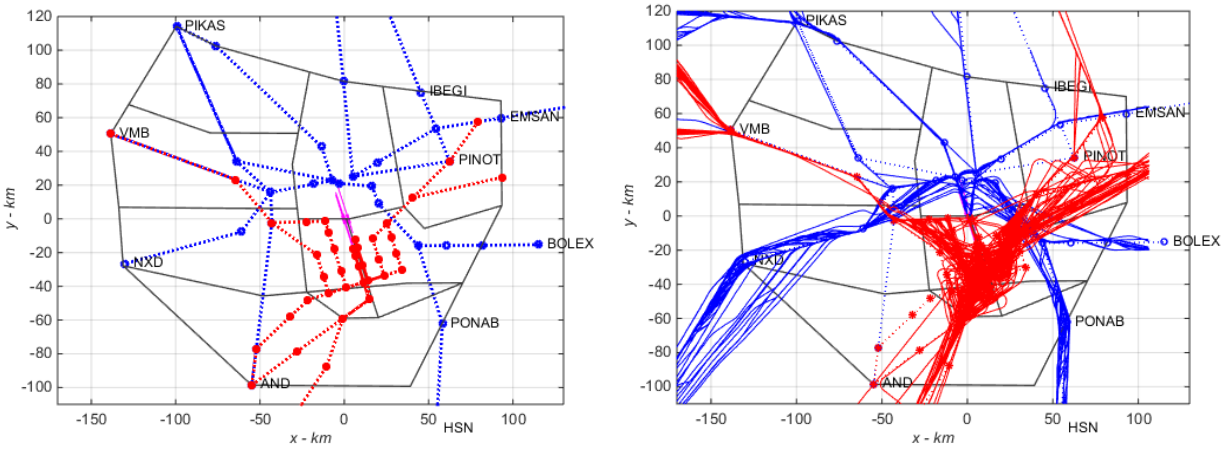

(a) SIDs, STARs and sectorization **(b) Radar Tracks on a particular day**

Figure 9 Diagram of the simulation scenario at ZSPD airport

At 6h UTC of the particular day (Jan. 2nd, 2013), wind field information were downloaded and decoded based on the steps described in subsection 3.1.4. And the wind speeds and directions at grids (0.75°×0.75°) were obtained by means of equation (5) and (6). Figure 10 provided the wind field in ZSSS TMA with 2D view and 3D view. Figure 10 (a) put the wind speeds and directions of the eight flight levels concerned all together on the horizontal view of terminal area, while Figure 10 (b) displayed the wind speeds and directions from the three dimensional perspective. Furthermore, the spatio-temporal interpolation was able to make the wind speed and direction available at particular position and fixed time for trajectory prediction.

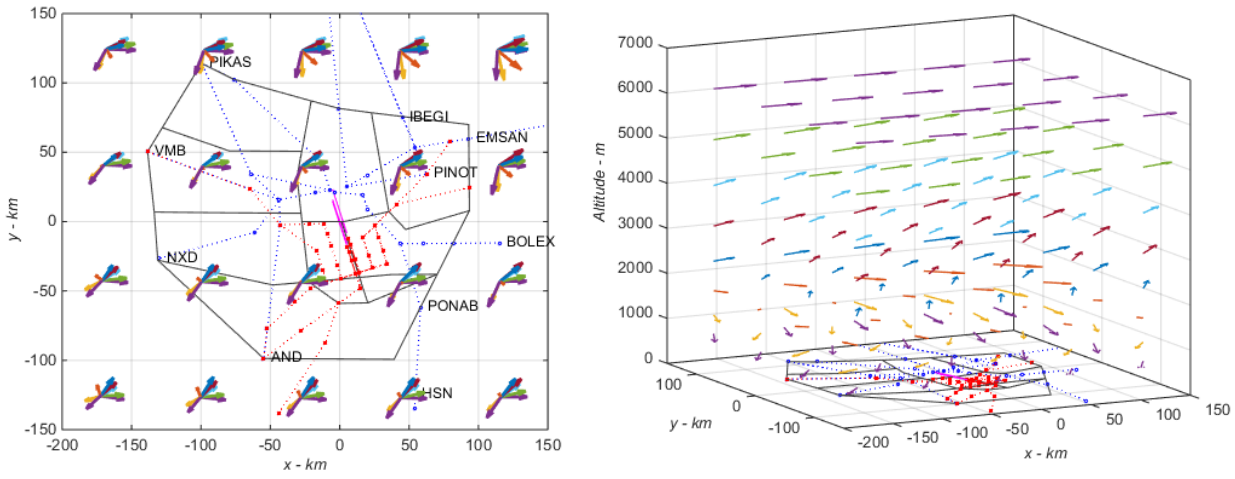

(a) 2D view **(b) 3D view**

Figure 10 Diagram of the wind field in ZSSS terminal area

4.1.1 Results

In this case, the most attention was paid to the validation of offline 4D-TP for departure aircraft. And the departure aircraft during one week operation through PIKAS-14X, a SID in ZSPD, were taken into account. The altitude profiles of those departures were shown in Figure 11. It could be seen from Figure 11 that different aircraft possessed unique climbing performance as the specific equipped engine and varied take-off weight. Under these conditions, the Boeing 737-800 series (B738) departure aircraft were considered in this case. Figure 12 presented the altitude profiles of B738 departures through PIKAS-14X. From this figure, we could find that the initial profiles were consistent with each other due to the similar climbing performance. However, after passing the second waypoint, the altitude profiles diverged as a result of typical transfer altitude given by controllers. Accordingly, we focused on the B738 departures through PIKAS-14X to Xi'an Xianyang airport (ZLXY), and the altitude profiles were shown in Figure 13. In this figure, the altitude profiles were similar to each other owing to these departure aircraft possessed the similar climbing performance and shared the same transfer altitude (9200 m).

In this case, CSN6437 was chosen to validate the performance of 4D-TP. CSN6437 was a B738 departure flight through PIKAS-14X to ZLXY in Jan. 2nd, 2013. The altitude profile of CSN6437 from radar track was blue line as shown in Figure 14. 4D-TP was carried out based on the computation model, performance parameters, aircraft intents and environmental conditions mentioned in subsection 3.1. The results of 4D-TP were also shown in Figure 14, in which the predicted altitude profiles with and without wind (using spatio-temporal interpolation based on the wind field, as shown in Figure 10) were denoted by black line and dotted black line respectively.

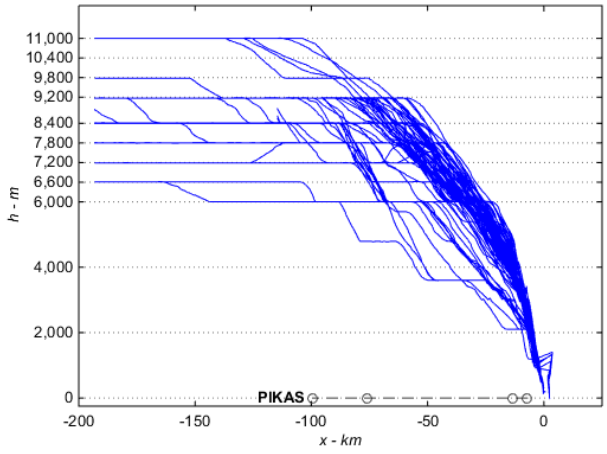

Figure 11 Altitude profiles through PIKAS-14X

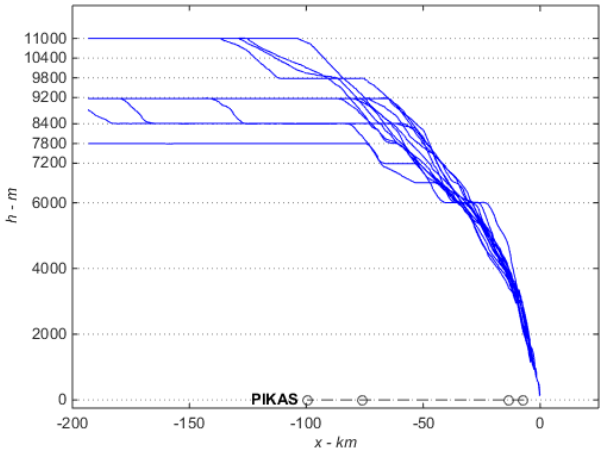

Figure 12 Altitude profiles of B738 through PIKAS-14X

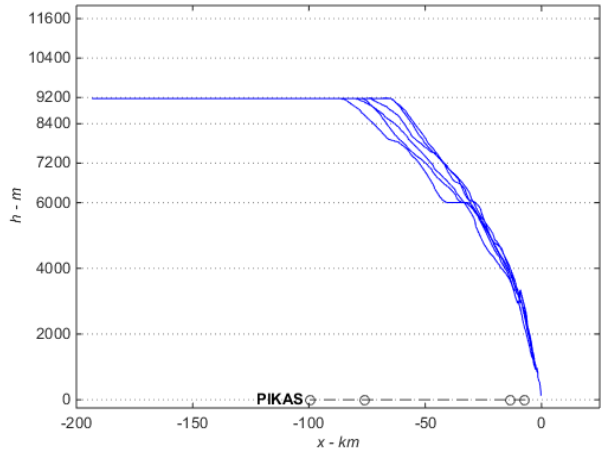

Figure 13 Altitude profiles of B738 to ZLXY

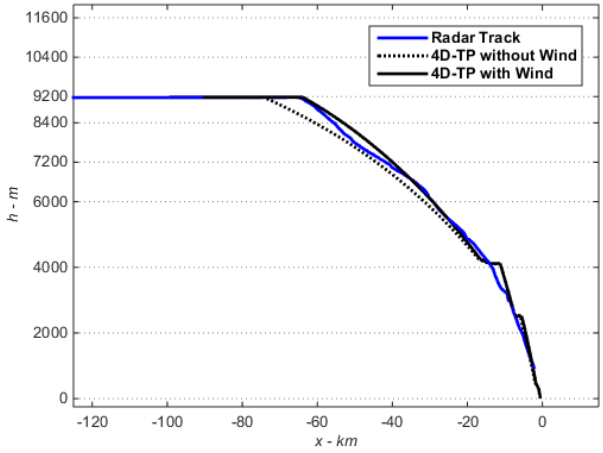

Figure 14 Altitude profiles of 4D-TP results of CSN6437

Furthermore, comparison between the actual time of arrival (ATA) and estimated time of arrival (ETA) at the waypoints was taken into consideration, while ATAs and ETAs were obtained from the radar tracks and the predicted results respectively. CSN6437 had passed PD061, PD062, PD064, NTG and PIKAS when flying through PIKAS-14X. And those ATAs and ETAs at such waypoints were listed in Table 3.

Table 3 Tabulation of flight time through the waypoints

Waypoints	Radar Tracks	TP without wind		TP with wind	
	t_{ATA} (s)	t_{ETA} (s)	error (s)	t_{ETA} (s)	error (s)
PD061	0	0	0	0	0
PD062	99	108	+9	110	+12
PD064	237	244	+7	252	+15s
NTG	732	682	-50	760	+28
PIKAS	882	798	-84	918	+36

4.1.2 Discussion

From Figure 14 and Table 3, several conclusions can be drawn as follows. Compared to the radar tracks, the proposed 4D-TP method could fulfill the trajectory prediction task well. Compared with 4D-TP without wind, 4D-TP with wind is able to improve the prediction accuracy. Besides computation model and performance parameters, aircraft intent and environmental condition are the key factors for 4D-TP.

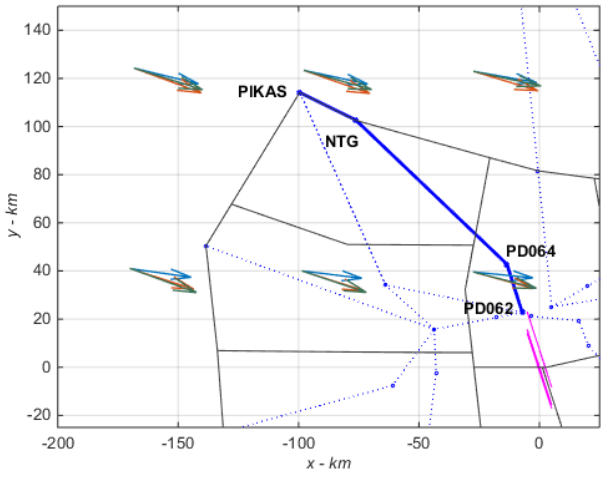

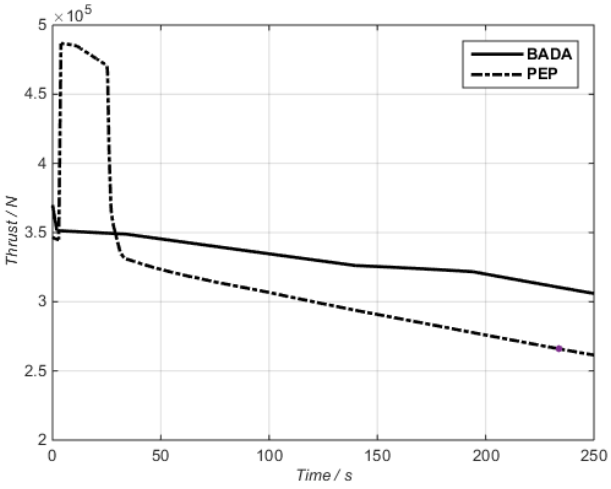

Figure 15 Diagram of the wind field around PIKS-14X **Figure 16 Diagram of comparison with thrust**

In this case, the transfer altitude is one kind of aircraft intent. If the transfer altitude is not available (as shown in Figure 11), accurate trajectory prediction becomes impossible. In addition, environmental condition is another key factor for 4D-TP. Figure 15 presents the wind field information around SID PIKAS-14X (blue line) during the operation time of CSN6437 at the altitude of 8000m, 8700m and 9400m. It can be seen from Figure 15 that CSN6437 encountered head wind during the climbing phase. As a consequence, the ETA at PIKAS of 4D-TP without wind is less than ATA at PIKAS and is also less than the ETA of 4D-TP with wind.

As to computation model and performance parameters, the former is dependent on the latter. That is to say, the available performance parameters restrict the computation model for 4D-TP. In our research, performance parameters from BADA have supported the Point-Mass Model for 4D-TP. As we have mentioned before, aircraft intent and environmental condition are the key factors for 4D-TP. In spite of that, computation model and performance parameters are the fundamental components of 4D-TP. It can

be seen from Figure 14 that during the initial climbing phase, the altitude profile of predicted results with or without wind is higher than the altitude profile of radar tracks. The reason seems to be obvious that the thrust computational equation and corresponding coefficients from BADA are too simplified. Since in BADA, the climb thrust is treated by multiplying maximum takeoff thrust with a ratio, which is dependent on aircraft mass. Figure 16 provides the comparison of thrust during the takeoff and initial climbing phases between BADA and PEP (Performance Engineer's Programs) software for Airbus 330-200 series aircraft under the same operational conditions. During the takeoff phase, thrust setting from PEP is greater than it from BADA, and the takeoff thrust setting from PEP only sustains less than one minute. During the initial climbing phase, thrust setting from PEP is smaller than it from BADA, which results in the steeper altitude profile of 4D-TP, as shown in Figure 14. Thereupon, computation model and performance parameters play a fundamental role in 4D-TP.

4.2 Online 4D-TP Case Study

In this case, we took Nanjing Lukou airport (ZSNJ) into consideration. And the operational scenario is shown in Figure 17. Figure 17 provided the SIDs, STARs and sectorization around ZSNJ airport, in which the grey lines represented sectorizaiton of the TMA, the blue and red dotted lines represented SIDs and STARs, respectively.

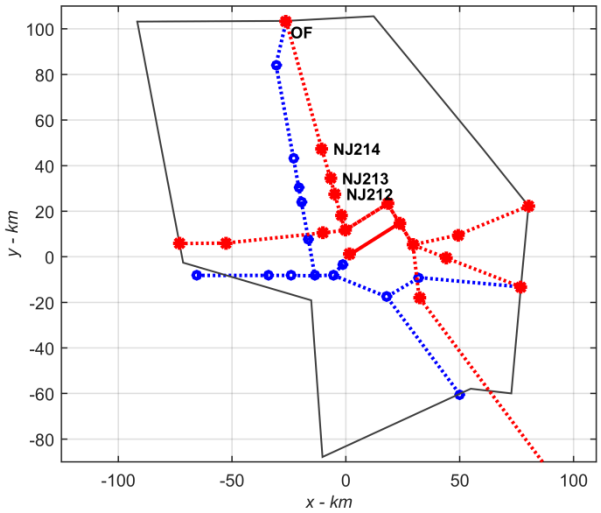

Figure 17 Diagram of the simulation scenario at ZSNJ airport

In this case, the most attention was paid to the validation of online 4D-TP for arrival aircraft through OF-42F, a STAR in ZSNJ. From Figure 17, we could find that OF-42F was composed of the following waypoints: OF, NJ214, NJ213, NJ212 and so on. The subsequent waypoints after NJ212 in OF-42F were out of the range of ADS-B receiver as it was located at our lab. Therefore, in this case, we focused on the comparison between ETAs (obtained from online 4D-TP) and ATAs (obtained from ADS-B receiver) at the following waypoints NJ214, NJ213, NJ212.

4.2.1 Results

For this validation, an online 4D-TP tool was developed using C++ programming language in the VS2005 and Qt4.5 development environment under Windows 7 operating system. Figure 18 presented the interface of the online 4D-TP tool, in which the dotted brown and green lines denoted STARs and SIDs of ZSNJ airport respectively, the grey lines represented the border of TMA, and the red line signified the preview of the online 4D-TP results. The arrival aircraft were denoted by red aircraft indicators, while departure and overfly aircraft by blue ones. The flight information (including flight ID, altitude, speed, aircraft type) was at the bottom-right of each aircraft indicator. The historical and predicted trajectory pointers were also provided by dashed and solid line with each aircraft indicator.

In this case, the pre-defined thresholds in Figure 7 were set as follows: Thr_Lateral = 3 km, Thr_Vertical = 300 m. If the deviation between the current states and predicted trajectories exceeded these pre-defined thresholds, trajectory re-prediction was triggered. And these pre-defined thresholds were variable system parameters, which could be changed according to the users' requirements.

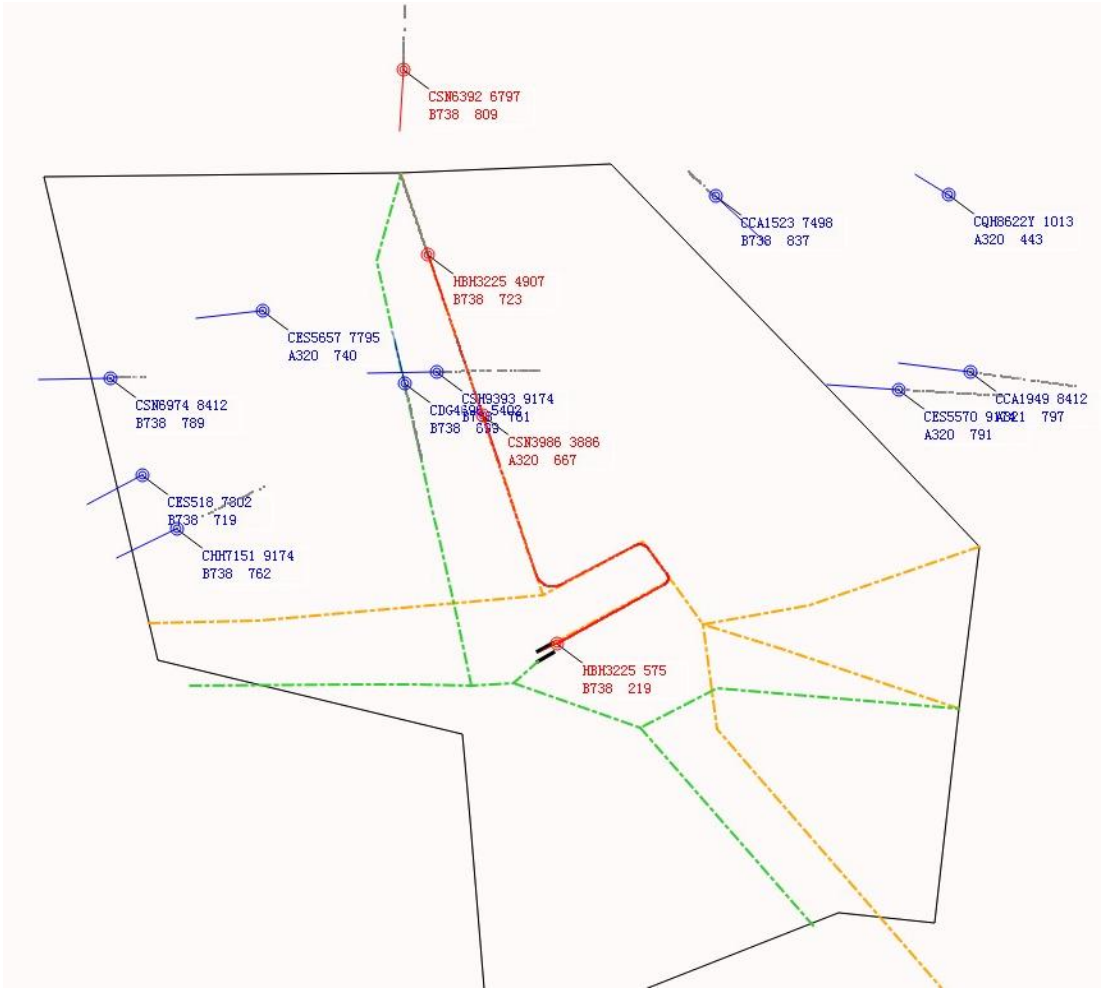

Figure 18 Diagram of interface of the online 4D-TP tool

Firstly, flight CXA8054, Boeing 737-800 from ZYCC (Changchun International Airport) to ZSNJ operated on July 8th, 2017, was chosen as the validation candidate. And the results of online 4D-TP were shown in Figure 19.

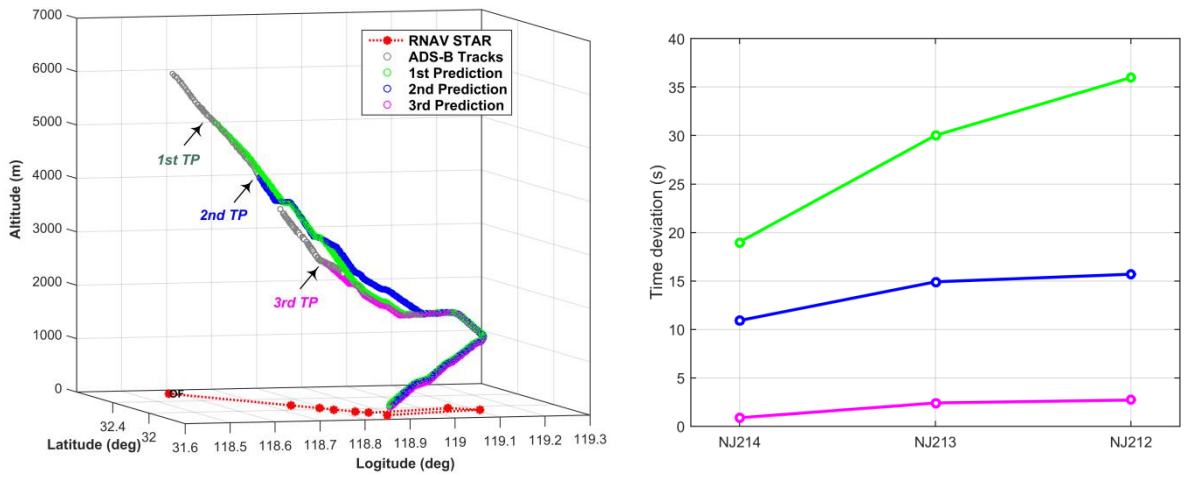

(a) Comparison of 3d tracks **(b) Deviation between ETAs and ATAs**

Figure 19 Results of Online 4D-TP for CXA 8054

Figure 19(a) presented the 3d tracks of CXA8054, including real tracks from ADS-B receiver and predicted trajectories from online 4D-TP tool, plus the RNAV STAR. Figure 19(b) provided the deviation between the ETAs and ATAs at different waypoints (NJ214, NJ213 and NJ212) during different predictions of 4D-TP. From Figure 19, we could find that the Trajectory Predictor had been triggered three times. The first predicted trajectory and time deviation are denoted by green lines, while the second predicted trajectory and time deviation by blue lines and the third by crimson lines. From Figure 19, we could also see that the latter TP was more accurate than the former one. That was owing to the aircraft intent updating strategy in our proposed online 4D TP method.

Secondly, 34 arrival flights landing on ZSNJ airport, operated from July 8thto July 10th, 2017, were taken into consideration for the online 4D-TP case study. Nearly one third of the flights were Boeing 737-800 type, while the others were Airbus 319/320/321. Figure 20 provided the frequency of 4D-TP triggering between Entry fix "OF" and Waypoint "NJ214". It should be noted that frequency "zero" in Figure 20 indicated that first Trajectory Prediction worked before "OF" was accurate enough.

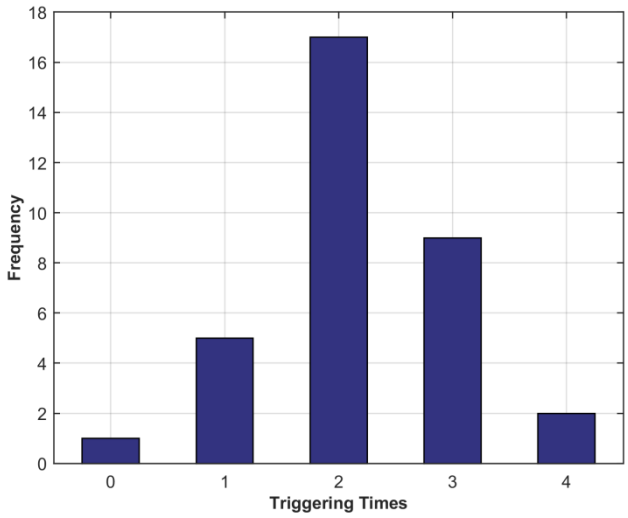

Figure 20 Frequency of 4D-TP triggering between OF and NJ214

From Figure 20, we could find the majority of triggering times of online 4D-TP for 34 arrival flights was around 1 to 3. Furthermore, nearly 80% of the total 74 triggering events were due to the vertical deviation between actual tracks and predicted trajectories exceeding the pre-defined 300 m. It implied that the aircraft vertical intent updating strategy played a key role in the online 4D-TP method.

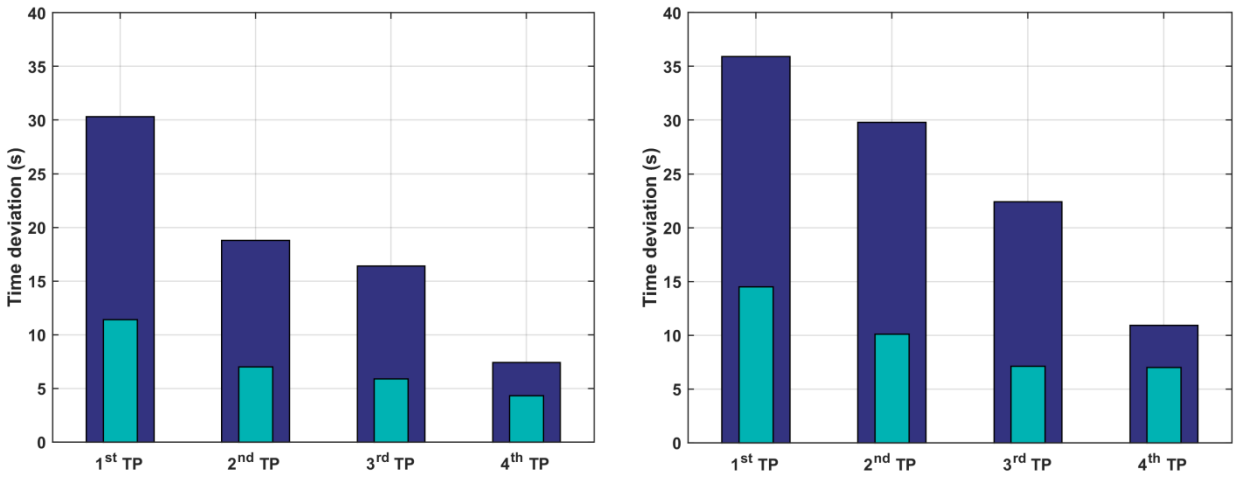

(a) at waypoint NJ213 **(b) at waypoint NJ212**

Figure 21 Time deviation between ETAs and ATAs

Thirdly, aiming at the total 74 triggering events mentioned above, we carried out the analysis of time deviation between ETAs and ATAs at Waypoint "NJ213" and "NJ212". Figure 21 presented the maximum and mean time deviation at "NJ213" and "NJ212".

In Figure 21, the outer bar was used to indicate the maximum time deviation between ETAs and ATAs, while the inner bar mean time deviation. It could be seen from Figure 21 that on the one hand, the further waypoint from current position led to the less accuracy of trajectory prediction; on the other hand, the later prediction brought about the better precision of trajectory prediction. In addition, we could find that flight CXA8054 was the worst case of the first Trajectory Prediction.

4.2.2 Discussion

As shown in Figure 19 and 21, the developed online 4D-TP tool was able to increase prediction accuracy by triggering 4D-TP while the position or speed error was beyond the pre-defined threshold. The value of pre-defined threshold had an influence on the triggering events of online 4D-TP. If a small threshold was defined, then the online 4D-TP might be activated frequently. Otherwise, the online 4D-TP might not be triggered in time. Furthermore, future work is required to design an appropriate index by considering those mentioned threshold simultaneously.

As for the flight CXA8054, we could find that the main reason for triggering Trajectory Predictor was the vertical deviation, as shown in Figure 19(a). Furthermore, as mentioned in section 4.2.1, nearly 80% of the total 74 triggering events were due to the vertical deviation. That was to say the vertical intent updating strategy played a key role in our proposed online 4D-TP method. Therefore, we used ten flights landing on ZSNJ airport on July 10th, 2017 to compare the prediction results of online 4D-TP with or without consideration of the vertical intent updating strategy.

Figure 22 presented the triggering frequency of online 4D-TP with and without consideration of the vertical intent updating strategy. In this figure, the yellow and blue bar were used to indicate the triggering frequency of online 4D-TP with and without consideration of the vertical intent updating strategy, respectively.

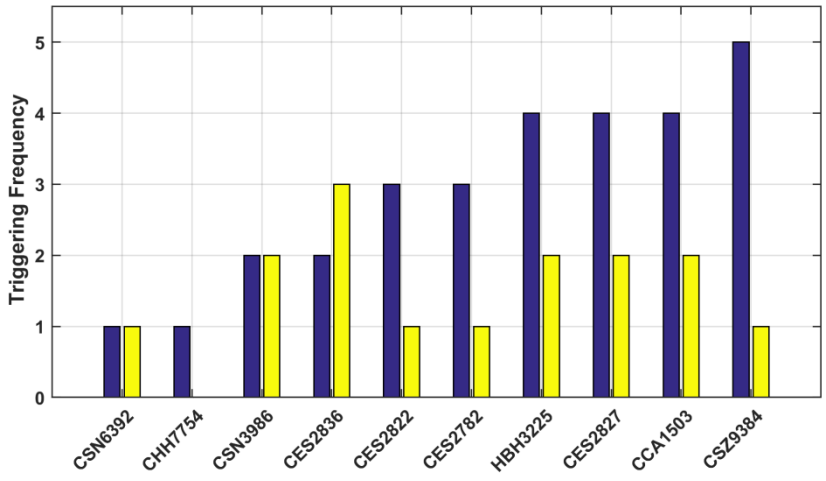

Figure 22 Frequency of 4D-TP triggering with and without vertical intent updating strategy

When taking vertical intent updating strategy into consideration, the total online triggered frequency of all flights was15, which was nearly half of the other case, 29. When considering the vertical intent updating strategy, only one of the whole 10 flights, CES2836, was required one more re-prediction. These observations indicated that the ETAs were changed less with consideration of the vertical intent updating strategy, which led to a better decision support could be made for controllers.

Furthermore, we tried to investigate the time deviation between the ETAs and ATAs with and without consideration of the vertical intent updating strategy. Figure 23 provided the prediction results about the two different scenarios.

In Figure 23, as before, the yellow and blue bar were used to indicate the mean time deviation of online 4D-TP with and without consideration of the vertical intent updating strategy, respectively. It should be noted that Figure 23(a) and 23(b) illustrated the time deviation of online 4D-TP per prediction and per flight, respectively. Namely, Figure 23(a) was obtained through total time deviations being divided by the whole number of predictions; while Figure 23(b) by the whole number of flights.

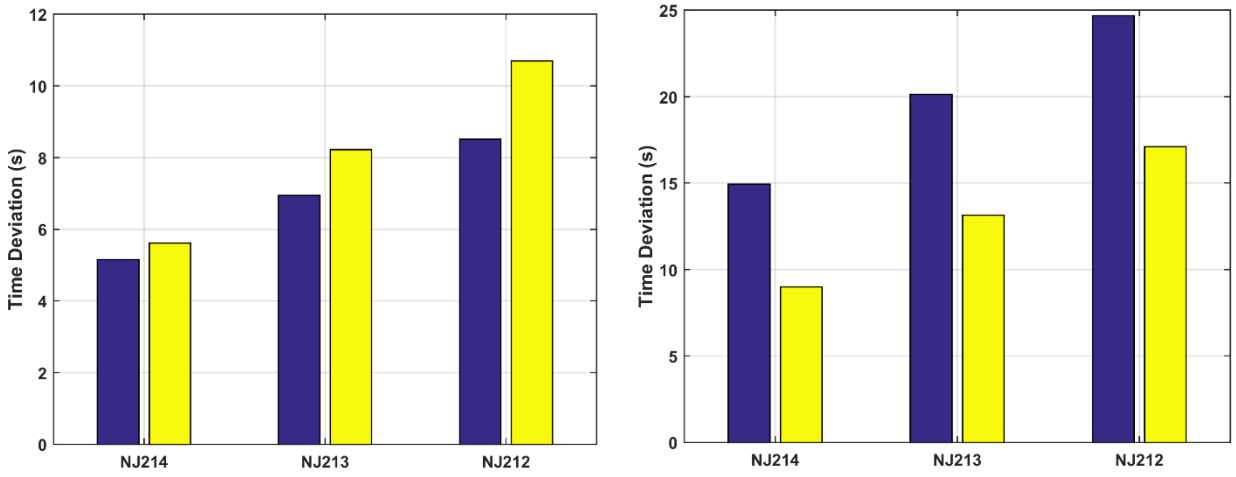

(a) per prediction **(b) per flight**

Figure 23 Time deviation between ETAs and ATAs with and without vertical intent updating strategy

As far as the first case is concerned, the prediction results of online 4D-TP with consideration of the vertical intent updating strategy were more than the other one. This was because the bigger divisor led to less value and the later prediction brought about the better precision. And as mentioned above, the more triggering events might result in a poorer decision support for controllers.

As far as the second case is concerned, the prediction results of online 4D-TP with consideration of the vertical intent updating strategy were better. The reason for this conclusion was twofold. One was owing to the less re-prediction times, viz. the smaller divisor. The other was due to the vertical intent updating strategy, which could make best use of the current flight mode to increase the prediction precision.

5. CONCLUSION

This paper has developed an online 4D-TP method, which is composed of preparation process, computation process and updating process. For online 4D-TP, the last process plays the most important role, including current trajectory updating and aircraft intent updating. By using the ADS-B Receiver, we could receive several messages. After message receiving, decomposing and decoding, the flight identification, position and velocity of every aircraft could be determined. Meanwhile, as to the updates of aircraft intent, including horizontal and vertical intent updating strategies, they are mainly dependent on the deviation between the current and predicted trajectory exceeding the pre-defined threshold whether or not.

This study has also carried out two types of case studies to demonstrate the performance and effectiveness of the proposed method: one is off-line 4D-TP by the radar tracks for the departure aircraft, and the other is online 4D-TP by the available current trajectory obtained from ADS-B receiver for the arrival aircraft. The following conclusions can be drawn from the present study: 1) computation model, performance parameters, aircraft intent and environmental condition are all the key factors for 4D-TP; 2)

the proposed online 4D-TP method is able to increase the prediction accuracy by triggering 4D-TP while the position or speed deviation is beyond the pre-defined threshold. 3) With consideration of vertical intent updating strategy, the online 4D-TP could reduce the re-prediction times while improving the prediction accuracy, which could help to make better decision support for controllers. Overall, this study serves as a basis and can also be applied to conflict detection, conflict resolution, aircraft sequencing and scheduling, etc.

However, BADA 3.12 is used in this paper for the point mass model, while BADA 4.x provides more enhanced model and increased levels of precision in aircraft performance parameters. Therefore, follow-up research could be launched by using BADA 4.x. Furthermore, the thrust setting should be addressed more properly. Thrust wanted model [32], considering the actual motion of the aircraft, maybe a viable alternative. And the “time-trigger mechanism” should be put into application to make the proposed online trajectory prediction method more applicable for conflict detection or arrival scheduling. Consequently, the further research should be undertaken in the following areas, like an appropriate index to trigger the re-prediction, applicable aircraft intent down-linked from the air [33] and some estimation methods for obtaining the aircraft parameters (like mass or thrust) [26, 27].

Conflict of interest statement

There is no conflict of interest regarding this journal article.

Acknowledgement

This work was supported by the National Science Foundation of China (71401072).

References

[1]. ICAO, Procedures for Air Navigation Services – Air Traffic Management, fifteenth ed., Doc.4444, Montreal, Canada, 2007.

[2]. Y. Matsunoa, T. Tsuchiyaa, J. Wei, I. Hwang, Stochastic optimal control for aircraft conflict resolution under wind uncertainty, Aerosp. Sci. Technol. 43 (2015) 77–88.

[3]. G. Solveling, J. P. Clarke, Scheduling of airport runway operations using stochastic branch and bound methods, Transp. Res., Part C, Emerg. Technol. 45 (2014) 119-137.

[4]. A. Gardi, R. Sabatini, S. Ramasamy. Multi-objective optimization of aircraft flight trajectories in the ATM and avionics context, Prog. in Aerosp. Sci. 83 (2016) 1-36.

[5]. FAA/EUROCONTROL COOPERATIVE R&D, Common TP structure and terminology in support of SESAR & NextGen. FAA/EUROCONTROL Action Plan 16, 2010.

[6]. L. Xie, J. F. Zhang, D. Sui, Aircraft track prediction based on interacting multiple model filtering algorithm, Aeronautical Computing Technique 5 (2012) 68-71.

[7]. I. Hwang, J. Hwang, C. Tomlin, Flight-mode-based aircraft conflict detection using a residual-mean IMM algorithm, in: AIAA Guidance, Navigation, and Control Conference and Exhibit, 2003, pp.1-11.

[8]. J. F. Zhang, X. G. Wu, F. Wang, Aircraft trajectory prediction based on modified interacting multiple model algorithm, J. Donghua Univ. 2 (2015) 180-184.

[9]. C. E. Seah, I. Hwang, Hybrid estimation algorithm using state-dependent mode transition matrix for aircraft tracking, in: AIAA Guidance, Navigation, and Control Conference and Exhibit, 2006, pp.1-15.

[10]. J. L. Yepes, I. Hwang, M. Rotea, New algorithms for aircraft intent inference and trajectory prediction, J. Guid. Control Dyn. 2 (2007) 370-382.

[11]. W. Y. Liu, I. Hwang, Probabilistic trajectory prediction and conflict detection for air traffic control, J. Guid. Control Dyn. 6 (2011) 1779-1789.

[12]. J. F. Zhang, D. Sui, X. M. Tang, Aircraft trajectory prediction based on SDTHE, System Engineering - Theory & Practice. 11 (2014) 2955-2964.

[13]. EUROCONTROL EXPERIMENTAL CENTER, User manual for the Base of Aircraft Data (BADA), revision 3.12, EEC Technical Report No.12/04, 2014.

[14]. L. A. Weitz, Derivation of a point-mass aircraft model used for fast-time simulation, MITRE Technical Report, MTR150184, 2015.

[15]. B. Zammit, D. Z. Mangion, Accuracy consideration of simple aircraft trajectory prediction model for idle thrust descent, in: 32nd Digital Avionics Systems Conference, 2013, pp.1E2-1 - 1E2-16.

[16]. M. Soler, A. Olivares, E. Staffetti, Multiphase optimal control framework for commercial aircraft four-dimensional flight-planning problems, J. Aircraft. 1 (2015) 274-286.

[17]. A. Franco, D. Rivas. Optimization of multiphase aircraft trajectories using hybrid optimal control, J. Guid. Control Dyn. 3 (2015) 452-467.

[18]. L. L. Javier. Definition of an aircraft intent description language for air traffic management applications, Ph.D. dissertation, Department of Aerospace Engineering, University of Glasgow, 2008.

[19]. J. A. Besada, G. Frontera, J. Crespo, et al, Automated aircraft trajectory prediction based on formal intent-related language processing, IEEE Trans. Intell. Transp. Syst. 3 (2013) 1067-1082.

[20]. X. M. Tang, P. Chen, Y. Zhang, 4D trajectory estimation based on nominal flight profile extraction and airway meteorological forecast revision, Aerosp. Sci. Technol. 45 (2015) 387-397.

[21]. J. W. Kampoom, W. Okolo, S. A. Erturk, et al, Wind field estimation and its utilization in trajectory prediction, in: AIAA Atmospheric Flight Mechanics Conference, 2015, pp.1-26.

[22]. EUROPEAN CIVIL AVIATION CONFERENCE, Report on standard method of computing noise contours around civil airports - Volume 1: applications guide, ECAC. CEAC Doc 29, 3rd Edition, 2005.

[23]. S. K. Hong, K. J. Lee, Trajectory prediction for vectored area navigation arrivals, J. Aerosp. Inf. Syst. 7 (2015) 1-13.

[24]. K. Tastambekov, S. Puechmorel, D. Delahaye, C. Rabut. Aircraft trajectory forecasting using local functional regression in Sobolev space, Transp. Res., Part C, Emerg. Technol. 39 (2014) 1-22.

[25]. A. Leege, M. Paassen, M. Mulder. A machine learning approach to trajectory prediction, in: AIAA Guidance, Navigation, and Control Conference, 2013, pp.1-14.

[26]. R. Alligier, D. Gianazza, N. Durand, Learning the aircraft mass and thrust to improve the ground-based trajectory prediction of climbing flights, Transp. Res., Part C, Emerg. Technol. 36 (2013) 45-60.

[27]. R. Alligier, D. Gianazza, N. Durand, Machine learning and mass estimation methods for ground-based aircraft climb prediction, IEEE Trans. Intell. Transp. Syst. 6 (2015): 3138-3149.

[28]. S. Vilardaga, X. Prats, P. Duan, et al, Conflict Free Trajectory Optimization with Target Tracking and Conformance Monitoring, in: AIAA Aviation Technology, Integration, and Operations Conference, 2014, pp.1-12.

[29]. R. Dalmau, R. Verhoeven, N. Gelder, X. Prats, Performance comparison between TEMO and a typical FMS in presence of CTA and wind uncertainties, in: 35th Digital Avionics Systems Conference, 2016, pp.1-8.

[30]. R. Dalmau, X. Prats, R. Verhoeven, et al, Performance comparison of guidance strategies to accomplish RTAs during a CDO, in: 36th Digital Avionics Systems Conference, 2017, pp.1-8.

[31]. TuDelft, ADS-B Decoding Guide. http://adsb-decode-guide.readthedocs.io/en/latest/index.html, 2015 (accessed Dec. 2nd, 2016).

[32]. M. Kaiser, M. Schultz, H. Fricke. Enhanced jet performance model for high precision 4D flight path prediction, in: ATACCS'11 Proceedings of the 1st International Conference on Application and Theory of Automation in Command and Control Systems, 2011, pp.26-27.

[33]. J. Bronsvoort, G. McDonald, M. Vilaplana, J. A. Besada, Two-stage approach to integrated air/ground trajectory prediction, J. Guid. Control Dyn. 6 (2014) 2035-2039.